Temperature dependence of the magnetic excitations in singlet-ground-state systems: Paramagnetic and zero-temperature behavior of Pr_3Tl and $(Pr, La)_3Tl$

T. M. Holden and W. J. L. Buyers
Atomic Energy of Canada Limited, Chalk River, Ontario, Canada
(Received 21 November 1973)

Neutron scattering experiments have shown that the magnetic excitations in polycrystalline $(Pr, La)_3Tl$ compounds are only weakly temperature dependent. This contrasts with the strong temperature renormalization predicted by the simple singlet-singlet and singlet-triplet models of induced moment systems. Calculations have been made of the spin-wave dispersion relation at zero temperature using the pseudoboson model and as a function of temperature in the paramagnetic phase using a generalized susceptibility theory including transitions between all levels of the ground multiplet. As the temperature increases it is found that mode-mode interaction between excitations out of the ground state and those out of excited states plays an important role. The temperature dependence of the excitations is found to be weak for most wave vectors and in agreement with experiment. Near the zone center where no experiments were possible the excitations are more strongly temperature dependent.

I. INTRODUCTION

There has been a growing interest in the magnetic properties of systems which possess a singlet ground state for which the ordering transition occurs by a magnetic polarization of the ground state. Reviews of this field have been given recently by Cooper[1] and Birgeneau.[2] Of particular interest and simplicity are the family of compounds based on Pr_3Tl in which the ground multiplet of the Pr ion ($J=4$) has a singlet Γ_1 state lowest, then a triplet Γ_4 followed by a doublet Γ_3, and a triplet Γ_5 state in cubic symmetry. The exchange interactions between the Pr ions in Pr_3Tl are only just sufficient to induce magnetic order at temperatures below 11.6 °K with an ordered moment of about one quarter of the maximum Pr moment.[3] Measurements of the spin-wave dispersion relation in polycrystalline material by neutron inelastic scattering have been made[3] and the unusual aspect of the experimental results was the insensitivity of the excitation energy to temperature. The experiments were performed at small scattering angles in order to obtain an average dispersion relation for the polycrystal and thus no results were obtained at wave vectors less than 0.3 Å^{-1}.

By contrast, theories with an approximate model Hamiltonian for Pr, that consists either of two singlet levels or of the lowest singlet and the first triplet[4] of the ground multiplet, predict a marked temperature dependence.

One obvious omission in the simple model theories is the neglect of the other levels belonging to the ground multiplet and this can be included within the many-level spin-wave model based on Grover's[5] pseudoboson theory which is satisfactory in the limit of $T=0$. This theory has been applied to $KCoF_3$,[6] TbSb,[7] and also to Pr_3Tl.[8] In the nonordered state the exchange-enhanced susceptibility of Peschel, Klenin, and Fulde,[9] which is analogous to the theory of paramagnons,[10] is valid. It may be applied if the exchange is not strong enough to produce magnetic order in singlet-ground-state systems or above the ordering temperature of materials which do become ordered. All levels of the lowest multiplet can be included in the calculation and the spectrum of excitations then includes excitations out of excited states which can mix with the usual spin waves out of the ground state.

From realistic calculations based on these theories we shall show that the marked contrast noted by Birgeneau *et al.*[3] between the experiment and the simple model theories comes from neglect in the theories of the higher energy levels and the excitations out of these excited states. The latter "excited state spin waves" are important for an understanding of the phase transition as we shall show in a following paper. In addition, most of the interesting temperature dependence is confined to wave vectors not accessible in powder experiments. In Sec. II the theory is outlined briefly and in Sec. III the numerical results are compared critically with experiment. The significance of the results is discussed in Sec. IV.

II. THEORY

A. Pseudoboson theory

The Hamiltonian describing the magnetic properties of the Pr ion is the sum of a single-ion part $\mathcal{H}_1$ and an interion exchange part $\mathcal{H}_2$. Thus

$$\mathcal{H}_1 = \sum_j h_1(j) ,$$

where

$$h_1 = B_4^0(O_4^0 + 5O_4^4) + B_6^0(O_6^0 - 21O_6^4) + B_2^0 O_2^0 + H_z S_z \quad (1)$$

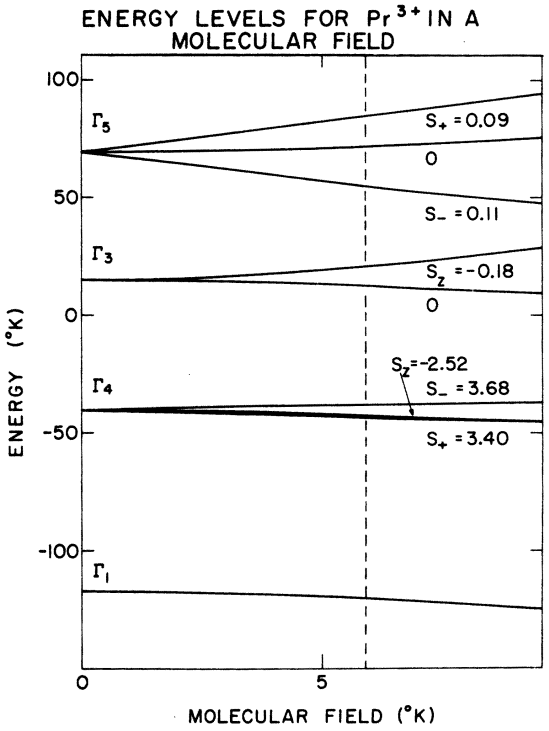

FIG. 1. Energy levels of the Pr^{3+} ion in a molecular field. The crystal-field-only states are denoted by their symmetry labels Γ_n. The broken vertical line gives the molecular field on the Pr^{3+} ion in Pr_3Tl at $T=0$ °K. For this molecular field the nonzero matrix elements of the total angular momentum $\vec{S}$ between the ground state 0 and each excited state n are given as S_α which is equal to the $S_{\alpha n0}$ defined in the text. Magnetic-dipole-inactive transitions from the ground state are denoted by a zero.

and

$$\mathcal{H}_2 = \sum_{j,j'} J(jj')\vec{S}_j \cdot \vec{S}_{j'} - \sum_j H_z S_{zj} . \tag{2}$$

Equation (1) includes the effect of a cubic crystal field with crystal-field parameters B_4^0, B_6^0 multiplying operator equivalents for $\vec{S}$, the total spin plus orbital angular momentum.[11] The effect of a tetragonal distortion is described by the B_2^0 term.

The single ion part of the exchange is written in terms of a molecular field H_z given by

$$H_z = 2\sum_{j'} J(jj')\langle S_{zj'}\rangle . \tag{3}$$

Equation (2) is the isotropic exchange interaction between ions at sites j and j' less the single ion part of the exchange already included in (1). $\mathcal{H}_1$ is solved self-consistently to find the eigenstates and the molecular field. The exchange mixing between the ground state and the excited states which gives rise to the induced moment and plays an important part in determining the energy gap at zero wave vector is thus included exactly for each atom. For the Pr_3Tl compounds the spin direction and hence the field H_z is directed along the edge of the cubic unit cell.

Figure 1 summarizes the effect of the molecular field on the energy levels which make up the ground multiplet with crystal-field parameters appropriate to Pr_3Tl. The exchange barely exceeds the critical value to induce a moment in the ground state. As a result the wave functions are little changed by the molecular field. The transfer matrix elements of $\vec{S}$ in zero molecular field and that appropriate to Pr_3Tl are compiled in Table I and are similarly little changed by the molecular field. The splitting between the ground state and the average of the first three excited states is increased by less than 3% in the molecular field.

The excitons at $T=0$ are described in terms of pseudoboson operators $a_m^\dagger$ which take an ion from the ground state to the mth excited state of the multiplet. In terms of these operators the angular momentum of an ion in the ground state at $T=0$ is given by

$$S_+ = \sum_m (S_{+m0}a_m^\dagger + S_{+0m}a_m) \tag{4}$$

and

$$S_z = S_{z00}\left(1 - \sum_m a_m^\dagger a_m\right) + \sum_m S_{zmm}a_m^\dagger a_m + \sum_m S_{zm0}(a_m^\dagger + a_m) , \tag{5}$$

where

$$S_{\alpha nm} = \langle n|S_\alpha|m\rangle \tag{6}$$

and $\langle n|S_\alpha|m\rangle$ is the matrix element of S_α evaluated between the single-ion states $|m\rangle$, $|n\rangle$ in the self-consistent molecular field. The single-ion Hamiltonian may be written in terms of the eigenvalues ω_m of the states $|m\rangle$ as

$$\mathcal{H}_1 = \sum_{j,m} (\omega_m - \omega_0) a_m^\dagger(j) a_m(j) . \tag{7}$$

All the terms which are nondiagonal in m come from the interion Hamiltonian $\mathcal{H}_2$ which, with Eqs. (4) and (5), takes the form for a ferromagnet

$$\begin{aligned}\mathcal{H}_2 = \sum_{jj'}\sum_{m,n} \{ &\tfrac{1}{2}J(jj')(S_{+m0}S_{-0n} + S_{-m0}S_{+0n})[a_m^\dagger(j)a_n(j') + a_m(j)a_n^\dagger(j')] \\ &+ \tfrac{1}{2}J(jj')(S_{+m0}S_{-n0} + S_{-m0}S_{+n0})[a_m^\dagger(j)a_n^\dagger(j') + a_m(j)a_n(j')] \\ &+ J(jj')S_{zm0}S_{z0n}[a_m^\dagger(j)a_n(j') + a_m(j)a_n^\dagger(j') + a_m^\dagger(j)a_n^\dagger(j') + a_m(j)a_n(j')]\} .\end{aligned} \tag{8}$$

TABLE I. Exciton energies and matrix elements of total angular momentum $\vec{S}$ in Pr_3Tl. The transitions important in the mode-mode interaction are indicated at the right. 1 THz is equal to 48.0 °K.

	Magnetic states						Nonmagnetic states						
n	Δ_n (THz)	$\langle n \mid S_z \mid n \rangle$	m	$\Delta_m - \Delta_n$ (THz)	$\langle m \mid S_\alpha \mid n \rangle$	α	n	Δ_n (THz)	$\langle n \mid S_z \mid n \rangle$	m	$\Delta_m - \Delta_n$ (THz)	$\langle m \mid S_\alpha \mid n \rangle$	α	
1	0.000	1.009	2	1.592	3.401	+	1	0.000	0.000	2	1.601	3.651	+	$\Gamma_4 - \Gamma_1$
			3	1.611	−2.523	z				3	1.601	−2.582	z	
			4	1.712	3.685	−				4	1.601	3.651	−	
			5	2.757	0					5	2.745	0		
			6	2.923	−0.186	z				6	2.745	0		
			7	3.650	0.115	−				7	3.882	0		
			8	3.995	0					8	3.882	0		
			9	4.262	−0.090	+				9	3.882	0		
2	1.592	0.650	3	0.018	1.932	−	2	1.601	0.500	3	0.000	0.707	−	$\Gamma_4 - \Gamma_4$
			4	0.119	0					4	0.000	0		
			5	1.164	3.995	+				5	1.144	3.742	+	$\Gamma_3 - \Gamma_4$
			6	1.331	−1.911	−				6	1.144	−2.160	−	
			7	2.058	0					7	2.280	0		
			8	2.403	−1.299	+				8	2.280	−1.871	+	
			9	2.669	−1.130	z				9	2.280	−1.323	z	
3	1.611	0.754	4	0.101	0.464	−	3	1.601	0.000	4	0.000	−0.707	−	$\Gamma_4 - \Gamma_4$
			5	1.146	0					5	1.144	0		$\Gamma_3 - \Gamma_4$
			6	1.312	−2.693	z				6	1.144	−3.055	z	
			7	2.039	−2.520	−				7	2.280	−1.871	−	
			8	2.384	0					8	2.280	0		
			9	2.651	1.151	+				9	2.280	1.871	+	
4	1.712	−0.256	5	1.045	3.450	−	4	1.601	−0.500	5	1.144	3.742	−	$\Gamma_3 - \Gamma_4$
			6	1.211	−1.994	+				6	1.144	−2.160	+	
			7	1.938	1.556	z				7	2.280	1.323	z	
			8	2.283	2.315	−				8	2.280	1.871	−	
			9	2.550	0					9	2.280	0		
5	2.757	0.795	6	0.167	0		5	2.745	0.000	6	0.000	0		
			7	0.893	1.818	+				7	1.136	1.414	+	
			8	1.238	−1.835	z				8	1.136	−2.000	z	
			9	1.505	0.913	−				9	1.136	1.414		
6	2.923	−1.763	7	0.727	1.966	−	6	2.745	0.000	7	1.136	2.449	−	
			8	1.072	0					8	1.136	0		
			9	1.338	2.778	+				9	1.136	2.449	+	
7	3.650	2.256	8	0.345	−3.382	−	7	3.882	2.5	8	0.000	−3.536	−	
			9	0.612	0.0					9	0.000	0		
8	3.995	−0.795	9	0.267	3.676	−	8	3.882	0.000	9	0.000	3.536		
9	4.262	−2.650					9	3.882	−2.5					

The solution in terms of plane waves follows the method of Walker[12] and leads to a secular matrix equation of dimension $2S \times 2S$ for a ferromagnet.

The theory includes the excitations out of the ground state to all excited states. The single-ion terms are treated exactly while the equations involving interionic exchange are linearized. In this theory excitations out of excited states are excluded. An even more restrictive condition is that, in order that the excitations $a_m^\dagger = C_m^\dagger C_0$ obey Bose commutation relations, all the ions must be in the ground state and the theory is thus valid only at $T = 0$.

B. Exchange-enhanced dynamical susceptibility

The derivation of the dynamical susceptibility for a paramagnet is sketched here. Full details will be given in a subsequent paper to be published on this topic.

At high temperatures one must project the spin operators into the full ground-state manifold:

$$S_+ = \sum_{n,m} S_{+mn} C_m^\dagger C_n \tag{9}$$

and

$$S_z = \sum_{n,m} S_{zmn} C_m^\dagger C_n \,, \tag{10}$$

where $C_n^\dagger$ is the operator which creates the single-ion state $|n\rangle$. The matrix elements $S_{\alpha mn}$ are determined as in Sec. II A. The corresponding energies of the states ω_n then appear as diagonal terms in the Hamiltonian. In the paramagnetic state the ω_n are the crystal-field-only energies and the Hamiltonian takes the form

$$\mathcal{H}_n = \sum_{j,n} \omega_n C_n^\dagger(j) C_n(j) + \frac{1}{2} \sum_{j,j'} J_{jj'} \times [S_+(j) S_-(j') + S_-(j) S_+(j') + 2 S_z(j) S_z(j')] \tag{11}$$

with the spin components given by (9) and (10).

It is convenient to introduce the dynamical susceptibility which, in the paramagnetic state of a cubic system, is the same for the three Cartesian spin components and in terms of the z component is

$$G(j, j', t) = -i\theta(t) \langle [S_z(j, t),\, S_z(j', 0)] \rangle \,. \tag{12}$$

The Fourier transform of $G(j, j', t)$ is

$$G(\vec{q}, \omega) = \sum_{j'} \frac{1}{2\pi} \int_{-\infty}^{+\infty} e^{i\omega t} G(j, j', t)\, dt\, e^{i\vec{q}\cdot[\vec{R}(j) - \vec{R}(j')]} \,. \tag{13}$$

The single-ion susceptibility obtained from the Heisenberg equation of motion by ignoring the second term in (11) will be denoted by $g(\omega)$ and is given by

$$g(\omega) = \sum_{n \neq m} \frac{S_{zmn} S_{znm} (f_m - f_n)}{\omega - \omega_n + \omega_m} \,. \tag{14}$$

The population of each state is $f_n = e^{(-\beta\omega_n)}/Z$ where $\beta = 1/kT$ and Z is the partition function. The equation of motion for $G(\vec{q}, \omega)$ involves higher-order Green's functions which are decoupled in the random-phase approximation

$$C_m^\dagger(j) C_s(j) C_q^\dagger(j') C_p(j') = \delta_{ms} f_m C_q^\dagger(j') C_p(j') + \delta_{qp} f_q C_m^\dagger(j) C_s(j) \tag{15}$$

to give the final result

$$G(\vec{q}, \omega) = g(\omega) [1 - 2J(\vec{q}) g(\omega)]^{-1} \,. \tag{16}$$

This simple form occurs in systems such as Pr^{3+}, Tb^{3+}, or Co^{2+} in a cubic field where the matrix elements are such that if S_{+mn} is not equal to zero then S_{+nm} and S_{znm} are zero. A simple generalization is possible to more complex systems like CoF_2 where the Co^{2+} ion is in a rhombohedral field. An alternative derivation of the dynamical susceptibility using a diagram technique has been given by Fulde and Peschel.[13] The Green's function $G(\vec{q}, \omega)$ is related to the usual measured dynamical susceptibility by

$$\chi(\vec{q}, \omega) = g^2 \mu_B^2 G(\vec{q}, \omega) \,. \tag{17}$$

The matrix elements $|S_{zmn}|^2$ used to calculate (17) have been conveniently tabulated by Birgeneau[14] for the paramagnetic phase. The neutron inelastic scattering cross section is proportional to

$$(1 - e^{(-\beta\omega)})^{-1} \operatorname{Im} \chi(\vec{q}, \omega).$$

The peaks in this cross section at a given wave vector occur at the energies of the excitons.

III. RESULTS

A. Pr_3Tl

The experimental energy-wave-vector-dispersion relation for polycrystalline Pr_3Tl determined by Birgeneau *et al.*[3] is shown in Fig. 2. Since the material is polycrystalline each point represents

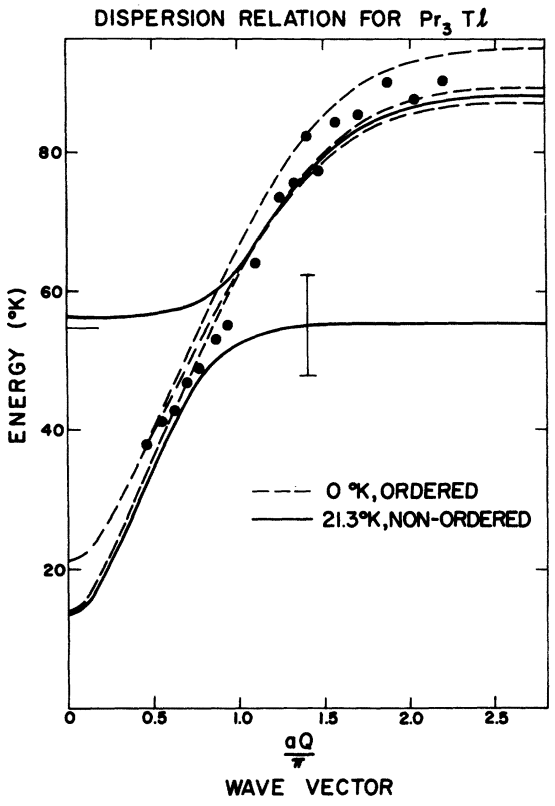

FIG. 2. Dispersion relation of magnetic excitons in Pr_3Tl. The neutron measurements of Birgeneau *et al.* (Ref. 3) (solid circles) on polycrystalline material at low temperature are to be compared with the average of the three broken lines obtained from the present pseudo-boson model. The full width of the observed neutron groups shown by the error bar indicates that the resolution of the spectrometer was insufficient to resolve the individual modes or branches near the crossover. Above T_c at $T = 21.3$ °K, which is $T/T_c = 1.28$ in terms of the theoretical transition temperature, the solid lines of the dynamical-susceptibility theory indicate that mode-mode interaction is important between the original singlet-triplet modes $\Gamma_4 - \Gamma_1$, and the excited-state modes associated with $\Gamma_3 - \Gamma_4$. The line at the left shows the position of the $\Gamma_3 - \Gamma_4$ transition in the high-temperature limit.

the spin-wave energy averaged over all directions in space corresponding to a given magnitude of wave vector. Because of the finite instrumental resolution each point is also an average over the first three branches of the dispersion relation.

The parameters used in the calculations will now be discussed. As pointed out by Birgeneau a close estimate of the average crystal-field splitting Δ between the ground state ω_1 and the first three excited levels ω_2, ω_3, ω_4 can be obtained from the measured energy at $aQ/\pi = 1.41$ since at this point contributions to the spin-wave energy from the transverse components of exchange are minimized and the effect on the spin-wave energy of the molecular field is small. Δ was found to be 77 °K. Although there is little physical justification for the procedure the ratio of B_4^0 to B_6^0 was fixed at the value predicted by the point-charge model (−149.4). The magnitudes of the crystal-field parameters B_4^0, B_6^0 are then chosen to reproduce the value observed for Δ and are found to be -4.97×10^{-2} °K and 3.33×10^{-4} °K, respectively. The exchange parameter[2] $J(-2.43\times10^{-1}$ °K) is chosen to give the observed ferromagnetic moment in Pr_3Tl at low temperatures.

The dispersion relations for the first two transverse branches and the first longitudinal branch of spin waves propagating in the $[\zeta, \zeta, 0]$ direction are shown by the dashed curves in Fig. 2. The frequencies were calculated from the pseudoboson model with the above exchange and crystal-field parameters. Note that the choice of wave vector along the $[\zeta, \zeta, 0]$ direction arises because the spin-wave energies averaged over all directions turn out to be close to those for the $[\zeta, \zeta, 0]$ direction for the same magnitude of wave vector.

Cooper[8] was the first to calculate the dispersion relation of Pr_3Tl in the pseudoboson model. We have repeated these calculations with the above exchange and crystal-field parameters and the results in Fig. 2 indicate an improved match between theory and experiment. Birgeneau[2] also compared the pseudoboson model with experiment with the above parameters and the curve in Fig. 6 of his paper is the average of the dashed curves in Fig. 2.

In the paramagnetic regime the same exchange and crystal-field parameters were used to calculate the dispersion relation using the exchange-enhanced susceptibility model, Eqs. (16) and (17). The result for $T = 21.3$ °K is shown as the solid curve in Fig. 2. In the paramagnetic regime a new mode appears corresponding to an excitation from the Γ_4 state to the Γ_3 state and the strength of the mode depends on the population of the Γ_4 state. When the energy of the spin wave out of the ground state equals the energy of this new mode, signified by a line in Fig. 2, resonant scattering and mode-mode repulsion occurs as shown in Fig. 2. The effect is absent at $T = 0$ because the population of the triplet state is zero. The effect is necessarily excluded in the singlet-singlet and singlet-triplet models since higher levels than the Γ_4 level are excluded.

In the experiment[3] it was not possible to observe the splitting due to mode-mode repulsion not only because of the averaging arising from use of a powder specimen but also because of the finite instrumental resolution. As shown by the error bar in Fig. 2 the experimental full width at half-maximum is considerably more than the splitting.

At low $\vec{q}$ the intensity is largely in the lower branch, whereas at wave vectors much larger than the wave vector, where the two branches would have crossed over in the absence of mode-mode repulsion, the intensity is largely in the upper branch. This behavior of the intensity is similar to that given in Fig. 4 for the dilute ferromagnet and so is not repeated here. This behavior indicates that in an experiment performed at low resolution such as that of Birgeneau *et al.*[3] a single branch of the dispersion relations (largely the three branches out of the ground state) would be observed with a rather smooth intensity variation. Only if the resolution was high enough would the second $\Gamma_3 - \Gamma_4$ peak be observed in the vicinity of the crossover.

At low resolution the experiment measures the average of the two solid curves weighted according to the intensity of each. We have calculated this average at one wave vector $aQ/\pi = 0.94$, where a series of measurements of the neutron group as a function of temperature were reported. This wave vector falls in the region where the mode-mode repulsion is strong. In Fig. 3 the energy corresponding to the mean energy of each neutron group[3] normalized to the energy at 4.4 °K is plotted against the temperature in units of the transition temperature. The solid curve in Fig. 3 is the theoretical temperature dependence of the average energy of the two branches of the dispersion relation weighted by the intensity of each as calculated from the dynamical-susceptibility model. The frequencies given by the dynamical-susceptibility model are normalized in Fig. 3 to the average frequency of the three lowest branches of the dispersion relation at zero temperature which is already known from our pseudoboson calculation. The dashed curve shows the reduced temperature dependence predicted within the singlet-singlet model evaluated with the same parameters Δ and J. Again the transition temperature predicted by the model was used to define the reduced temperature scale. It is clear that the inclusion of the higher levels in the present dynamical-susceptibility model substantially improves the agreement of theory with experiment.

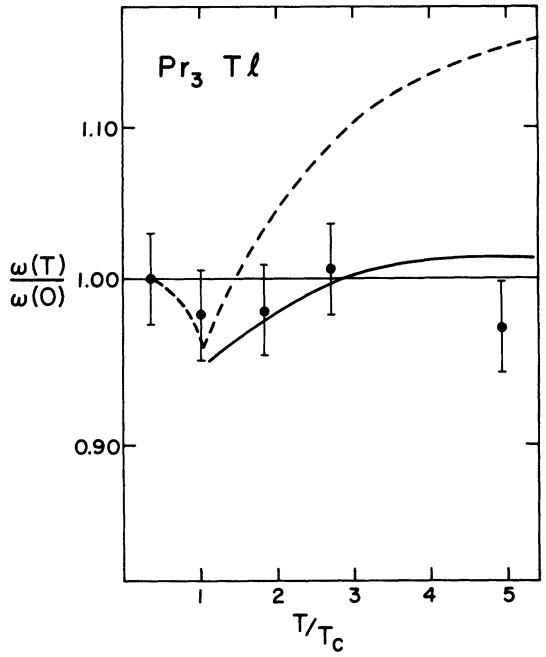

FIG. 3. Temperature dependence of the magnetic excitons in Pr_3Tl according to experiment (Ref. 3) (circles), singlet-singlet model (broken line), and the present dynamical-susceptibility theory (solid line).

B. $(Pr_{1-x}La_x)_3Tl$ compounds

In order to pass from the situation where the exchange is just sufficient to induce magnetic ordering to that where no ordering occurs, Birgeneau *et al.*[2,3] also studied the $(Pr, La)_3Tl$ compounds where nonmagnetic La replaces Pr substitutionally. Magnetization studies[15] show that these compounds do not order for La concentrations greater than about 7%. Detailed measurements of the dispersion relation of $(Pr_{0.88}La_{0.12})_3Tl$ were made with results shown in Fig. 4. Measurements of the neutron group at $aQ/\pi = 0.94$ were made over the temperature range 4.5–110 °K.

The effect of introducing nonmagnetic defects into an induced moment system is likely to be complicated. The static disturbance is probably long-ranged since the absence of a moment on the nonmagnetic La site will depress the induced moment at the surrounding sites. The defect modes will be resonant in character and their calculation will involve a complex self-consistency problem.[16] The simplest approach in analyzing polycrystalline data[2] is to reduce the exchange parameter by the percentage of La in the alloy, a procedure which gives the correct average behavior for dilute insulating magnets.[17] Since the lattice parameter only changes by 0.1% on going to the La-doped alloy the same crystal-field parameters were retained for the Pr ion.

The dispersion relation at 0 °K for propagation in the $[\zeta, \zeta, 0]$ direction with J reduced by 12% of its value in Pr_3Tl, calculated from the pseudoboson model is shown as the solid line in Fig. 4, which agrees fairly well with experiment. The dispersion relation calculated from the generalized-susceptibility model gives an identical result as expected at $T = 0$. The dashed curve and the dotted curve in the upper part of Fig. 4 show the dispersion relation at 33 and 110 °K calculated from the dynamical susceptibility and these curves show the same mode-mode repulsion features found earlier. The arrow gives the energy separation of the Γ_4 and Γ_3 levels. The calculated intensity

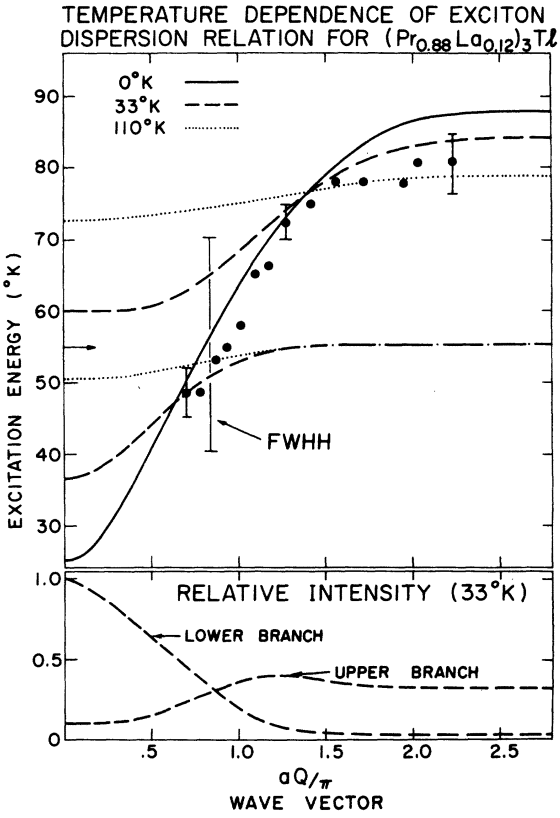

FIG. 4. In the upper part the dispersion relations for $(Pr_{0.88}La_{0.12})_3Tl$ calculated from the dynamical-susceptibility theory are given for three temperature. The 0 °K results (solid line) are to be compared with the neutron measurements of Birgeneau *et al.* (Ref. 3) (solid circles). The long error bar shows that the full widths at half-height (FWHH) of the observed neutron groups were such that, in the region of the crossover, the spectrometer averaged over both the branches of the dispersion relation that are present at high temperatures. The lower part of the figure shows how the intensity of the neutron scattering is mainly from the lower branch of the dispersion relations at small wave vectors and mainly from the upper branch at large wave vectors. The arrow at the left indicates the energy of the $\Gamma_3 - \Gamma_4$ transition in the high-temperature limit.

of the modes for 33 °K is shown in the lower part of Fig. 4. The lower branch has high intensity at small wave vectors while the upper branch has low intensity, but beyond the mode-splitting region the upper branch is more intense than the lower. As the temperature is raised the mode-mode repulsion increases; in addition, the wave-vector dependence of the two branches decreases.

As for Pr_3Tl the detailed temperature-dependence study was conducted in the region of the mode repulsion. Figure 5 shows the temperature dependence of the mode at $aQ/\pi = 0.94$ normalized to the energy at 4.5 °K. The dashed curves show the temperature dependence of the upper and lower modes at this wave vector. Since the experimental full width at half-maximum is greater than the maximum splitting, one would expect to observe the weighted average of the upper and lower modes and this is given by the solid curve in Fig. 5. The predictions of the singlet-singlet and singlet-triplet models are also shown in Fig. 5. The present theory based on the dynamical susceptibility is seen to be in better agreement with experiment than either of the other two models. The dynamical susceptibility also predicts a temperature dependence of the exciton intensity that is in qualitative agreement with the intensity decrease found experimentally.

C. Face-centered cubic Pr

Face-centered cubic Pr does not follow the pattern of the Pr_3Tl compounds. The spin-wave energy[3] at $aQ/\pi = 1.41$ is very nearly the same as for the compounds; from the measured energy at this wave vector one concludes that the average splitting between the ground state and the first three excited states is within 2% of the value for the compounds. However, the wave-vector dependence of the spin-wave energies is less than for the compounds and corresponds to an exchange parameter which is roughly 0.6 of that for Pr_3Tl. With this magnitude of exchange parameter it is found that, within molecular field theory, there should be no magnetic order in the system. Experimentally, however, fcc Pr does appear to order in the polycrystalline state with a moment of about $0.7\mu_B$ at a temperature of about 20 °K. However, the magnetization determined by neutron diffraction[3] has an unusual shape and shows no evidence for the 8.7 °K transition found in bulk magnetization studies.[18] Thus it is not possible to understand the magnetism of fcc Pr with cubic-crystal-field parameters and a single-exchange constant, and a level scheme as in Fig. 1. The effect of a B_2^0 term to simulate tetragonal-lattice distortion was examined, but it was found that if B_2^0 was chosen large enough to give the observed magnetic moment, the splitting between the first excited state of the triplet and the next two excited states is found to be large and would have been experimentally observable. No attempt has therefore been made to develop a model for pure praseodymium.

IV. DISCUSSION AND CONCLUSIONS

The results show that the dynamic susceptibility gives a good description of the observed temperature dependence of the neutron-inelastic scattering. The weak temperature dependence observed for the spin-wave mode at $0.94(\pi/a)$ is thus seen to be partially a result of the averaging performed by the spectrometer over the modes in the neighborhood of the mode-mode repulsion. At larger wave-vector transfers, say $2\pi/a$, the neutron scattering will be from the upper of the two modes in Fig. 4. This mode only falls by 3% between 0 and

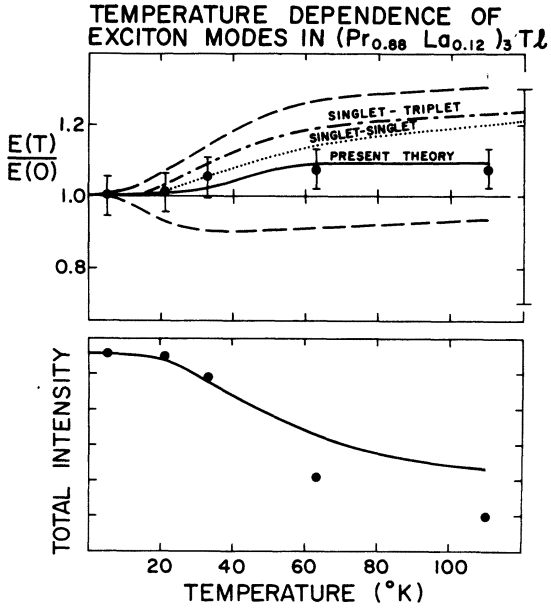

FIG. 5. Upper figure shows temperature dependence of the energy of the neutron group $E(T)$ observed at $aQ/\pi = 0.94$ in $(Pr_{0.88}La_{0.12})_3Tl$ relative to its energy $E(0)$ at $T = 0$ °K. Experimental results (solid circles) are compared with predictions of three theories. Upper (lower) unlabeled broken curve shows prediction of present dynamical-susceptibility theory for the temperature dependence of the mode from the upper (lower) branch of the dispersion relations. Weighted average of these two curves gives the solid line for comparison with experiment. The presence of other branches of the dispersion relation and consequent mode-mode interaction are ignored in the singlet-singlet and singlet-triplet theories. Lower figure shows how the observed neutron intensity (arbitrary units) is predicted on the present theory to fall with temperature. Solid circles were obtained by measuring the areas under the neutron groups and are of unknown accuracy since parts of the published neutron groups were an extrapolation of the data (see Fig. 8 of Ref. 2).

33 °K. We conclude that the temperature dependence of the larger wave-vector modes is also relatively weak.

Most of the rapid temperature dependence occurs for modes at small wave vectors that are inaccessible in the powder experiment; for example, the $Q = 0$ mode rises by about 50% between 0 and 33 °K. The reason that the long wavelength modes are more sensitive to temperature than the zone-boundary modes may be understood from the dynamical-susceptibility theory. Assume that, of the excited states, only the Γ_4 state has appreciable population. If the Γ_1 state has population f_1 and each Γ_4 state has population f_2, then the single-ion response is

$$g(\omega) = \frac{2\Delta\,|\langle\Gamma_4|S_z|\Gamma_1\rangle|^2(f_1 - f_2)}{\omega^2 - \Delta^2} \quad .$$

The renormalized response (16) then gives the exciton frequencies as

$$\omega(\vec{q}) = \{\Delta[\Delta + 4J(\vec{q})\,|\langle\Gamma_4|S_z|\Gamma_1\rangle|^2(f_1 - f_2)]\}^{1/2} \quad .$$

The small frequency at the zone center occurs because $J(0)$ is negative and, when multiplied by the population factor and the matrix element, almost cancels the Δ in the square bracket. A small increase in the population factor f_2 of the Γ_4 states thus produces a much larger effect on $\omega(\vec{q})$. At the zone boundary $J(\vec{q})$ is positive and the second term adds to the Δ. Thus a small change in f_2 produces only a small change in the square bracket and consequently on $\omega(\vec{q})$. The long wavelength modes are therefore especially sensitive to temperature in an induced-moment system if they have low frequencies. The effect for the induced ferromagnet is quite different to the effect for a normal ferromagnet below T_c with a large anisotropy gap Δ', where one has schematically for $S = \frac{1}{2}$, $\Delta = \Delta' - 2SJ(0)$, so that

$$\omega(\vec{q}) = \Delta' - 2\langle S\rangle[J(0) - J(\vec{q})] \quad .$$

In this case any effective renormalization of the spin is absent at the zone center and a maximum at the zone boundary.

It is of interest to consider why the random-phase approximation appears to work successfully in the present case. The reason is likely that the fluctuating-exchange fields in the disordered state do not markedly affect the energies or wave functions of the crystal-field states. The effect of the full molecular field on the wave functions, although crucial, can be seen from Table I to be small and similarly the induced splitting in Fig. 1 is small. It follows that there will probably not be much scattering of the mean-field magnetic excitons. The theory may be less useful for systems where the exchange field exceeds by a large factor the critical field required to produce long-range order as it does by a factor of more than 3 in the case of TbSb.[7] In that case the energies and wave functions are greatly altered by the exchange field.

An alternative explanation of the temperature dependence of the spin-wave energies in Pr_3Tl has recently been proposed by Hoenerlage[19] which involves a magnon-phonon interaction at the point at which the $\Gamma_4 - \Gamma_1$ branch of the dispersion relation and a transverse phonon would intersect. As the phonon-dispersion relation is unknown for Pr_3Tl it is not possible to examine this suggestion quantitatively at present. However, it is probably true that a complete understanding of the properties of materials such as Pr_3Tl containing rare-earth ions will require taking static and dynamic distortions of the crystal lattice into account.

Further work is underway to generalize the dynamical-susceptibility approach to treat the case of elevated temperatures within the ordered phase. Experimental work is required to check the details of the theory. Experiments on single-crystal samples at high resolution are especially desirable to observe the mode-mode repulsion and $q = 0$ behavior directly.

[1] B. R. Cooper, in *Magnetic Properties of Rare Earth Metals*, edited by R. J. Elliott (Plenum, London, 1972), p. 17.

[2] R. J. Birgeneau, AIP Conf. Proc. 10, 1664 (1973).

[3] R. J. Birgeneau, J. Als-Nielsen, and E. Bucher, Phys. Rev. Lett. 27, 1530 (1971); Phys. Rev. B 6, 2724 (1972).

[4] Y. L. Wang and B. R. Cooper, Phys. Rev. 185, 696 (1969); D. Pink, J. Phys. C 1, 1246 (1968).

[5] B. Grover, Phys. Rev. 140, A1944 (1965).

[6] W. J. L. Buyers, T. M. Holden, E. C. Svensson, R. A. Cowley, and M. T. Hutchings, J. Phys. C 4, 2139 (1971).

[7] T. M. Holden, E. C. Svensson, W. J. L. Buyers, and O. Vogt, in *Neutron Inelastic Scattering* (IAEA, Vienna, 1972), p. 553.

[8] B. R. Cooper, Phys. Rev. B 6, 2730 (1972).

[9] I. Peschel, M. Klenin, and P. Fulde, J. Phys. C 5, L194 (1972).

[10] N. F. Berk and J. R. Schrieffer, Phys. Rev. Lett. 17, 433 (1966); S. Doniach and S. Engelsberg, Phys. Rev. Lett. 17, 750 (1966).

[11] M. T. Hutchings, in *Solid State Physics*, edited by F. Seitz and D. Turnbull (Academic, New York, 1964), p. 227.

[12] L. R. Walker in *Magnetism*, edited by G. T. Rado and H. Suhl, (Academic, New York, 1963), Vol. 1, p. 299.

[13] P. Fulde and I. Peschel, Z. Phys. 241, 82 (1971).

[14] R. J. Birgeneau, J. Phys. Chem. Solids 33, 59 (1972).

[15] K. Andres, E. Bucher, S. Darack, and J. P. Maita, Phys. Rev. B 6, 2716 (1972).

[16] R. A. Cowley and W. J. L. Buyers, Rev. Mod. Phys. 44, 406 (1972).

[17] E. C. Svensson, T. M. Holden, W. J. L. Buyers, R.

A. Cowley, and R. W. H. Stevenson, Solid State Commun. 7, 1693 (1969).
[18]E. Bucher, C. W. Chu, J. P. Maita, K. Andres, A. S. Cooper, E. Buehler, and K. Nassau, Phys. Rev. Lett. 22, 1260 (1969).
[19]B. Hoenerlage, Z. Phys. 260, 403 (1973).